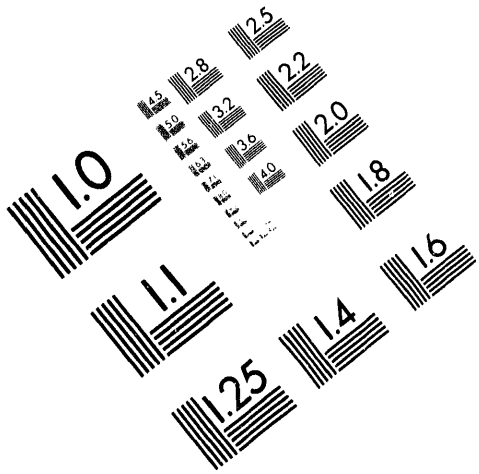

Association for Information and Image Management
1100 Wayne Avenue, Suite 1100
Silver Spring, Maryland 20910
301/587-8202

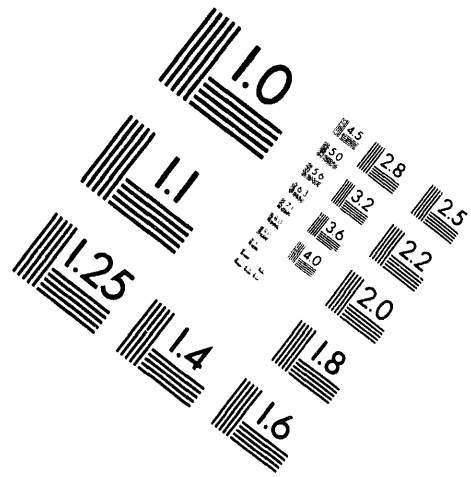

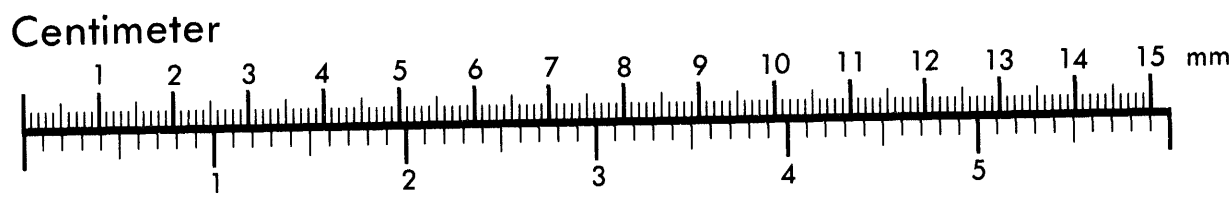

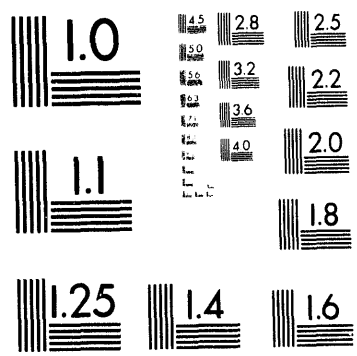

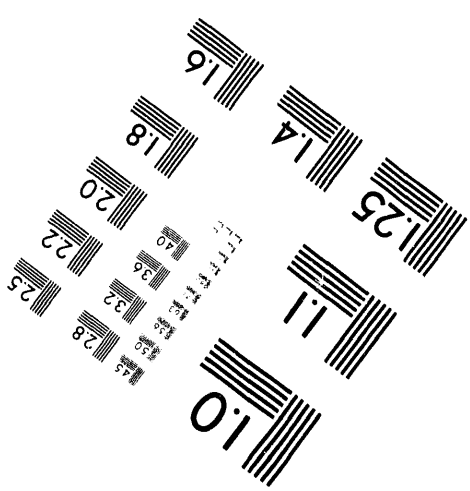

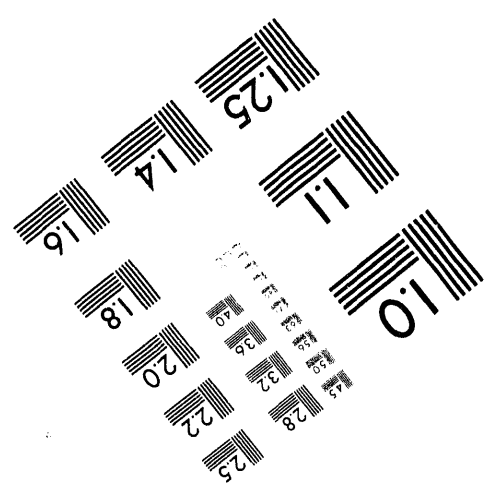

MANUFACTURED TO AIIM STANDARDS
BY APPLIED IMAGE, INC.

1 of 1

To be presented at the ABAQUS Users' Conference in Newport, Rhode Island on June 1-3, 1994.

SAND93-3949C

Conf-9406132--2

Analysis of Concrete Containment Structures under Severe Accident Loading Conditions*

Vicki L. Porter
Engineering Mechanics and Material Modeling Department 1561
Sandia National Laboratories
Albuquerque, NM

Abstract

One of the areas of current interest in the nuclear power industry is the response of containment buildings to internal pressures that may exceed design pressure levels. Evaluating the response of structures under these conditions requires computing beyond design load to the ultimate load of the containment. For concrete containments, this requirement means computing through severe concrete cracking and into the regime of wide-spread plastic rebar and/or tendon response. In this regime of material response, an implicit code can have trouble converging. This paper describes some of the author's experiences with Version 5.2 of ABAQUS Standard and the ABAQUS concrete model in computing the axisymmetric response of a prestressed concrete containment to ultimate global structural failure under high internal pressures. The effects of varying the tension stiffening parameter in the concrete material model and variations of the parameters for the ***CONTROLS** option are discussed.

*This work was performed at Sandia National Laboratories, Albuquerque, New Mexico, supported by the United States Department of Energy under Contract DE-AC04-94AL85000.

Introduction

Finite element methods for structural analysis have long been a mainstay in the design of containment structures for the nuclear power industry. Due to very stringent design guidelines, these analyses were limited to design pressures with very conservative factors of safety. Therefore, the traditional finite element computations were always in the elastic regime. However, in recent years, the nuclear power industry and government agencies have begun to investigate the response of containment structures to much higher internal pressures that could be encountered during a severe accident. Under these loading conditions, nonlinear response of the containment vessel is highly probable.

This paper describes finite element analyses using ABAQUS/Standard Version 5.2 [1] performed at Sandia National Laboratories for the response of a prestressed concrete containment vessel under severe internal pressure loading. One of the goals of this program is the validation and verification of existing finite element technology for predicting behavior in the non-linear regime and, ultimately, for predicting failure. This requires the finite element code to be able not only to predict cracking of the concrete, but also to continue the analysis through large plastic deformation of the reinforcing steel and/or tendons.

Problem Description

A simplified schematic of a prestressed concrete containment vessel is shown in Figure 1. The interior wall and floor of the containment vessel are lined with steel. The prestressing system consists vertical hairpin tendons with ends anchored in the tendon gallery at $180°$, and hoop tendons anchored in each of two buttresses located $180°$ apart.

Finite element analyses were conducted to obtain the global, axisymmetric deformation of the containment. The finite element model used is shown in Figure 2. A $20°$ slice of the structure was modeled with axisymmetric boundary conditions on the planes at $\theta = 0°$ and $\theta = 20°$. The

finite element model consists of 1160 four-noded shell elements and 3225 8-noded bricks. The dome and cylindrical wall are modeled with composite shell elements consisting of a thin inner layer of steel representing the liner and a much thicker outer concrete layer. The steel liner along the floor is modeled with shell elements whose nodes are equivalenced with those of the hexahedral elements composing the basemat. Shell elements are also used to line the top surface of the tendon gallery to provide an anchor for the vertical tendons.

All rebar in the containment vessel was modeled using the rebar subelements. Tendons and liner anchors in the hoop and meridional directions were also modeled as rebar. Prestressing was induced in the tendons with use of the ***INTIAL CONDITIONS** option. Modeling the tendons as rebar subelements implies that the tendons are bonded to the concrete. That is, slippage of a tendon within the tendon sheath is not considered.

Structural loads imposed on the containment vessel include gravity, foundation pressure, and internal pressure. The basemat foundation was modeled with the ***FOUNDATION** load type. During an initial load step, the containment is brought into equilibrium under the prestressing and gravity loads only with no internal pressure. In subsequent steps, the internal pressure is gradually applied.

All steel components of the structure were modeled as elastic-plastic with hardening. The concrete was modeled with the concrete model included in ABAQUS/Standard with default failure ratios. The ***TENSION STIFFENING, TYPE=STRAIN** parameter was varied from 0.001 to 0.003 in order to investigate its influence on the results and on the convergence behavior of the code. All analyses were run on a CRAY YMP 8/64.

Results

Figure 3 shows the distribution of hoop strain in the wall of the containment at internal pressures of 1.0 and 1.29MPa, respectively. At 1.0 MPa, the concrete has cracked and the steel liner has

yielded throughout the length of the containment wall from the basemat to the springline. At this pressure, all the tendons and the rebar are still elastic. By an internal pressure of 1.2MPa, however, the hoop rebar has begun to yield, and by 1.3 MPa yielding has begun in the hoop tendons. Note that at the higher pressure, the deformation is no longer axisymmetric even though axisymmetric boundary conditions have been applied to the edges. Once the rebar has yielded in an element, it undergoes more rapid hoop strain than its neighboring elements. In this case, the hoop strain is approximately the same at both edges and the center, with lower values in the intermediate elements. (Ten elements were used in the circumference of the 20° section.)

Hoop strain histories for three different analyses are shown in Figure 4. The values indicated for tension stiffening are the strains at which the tensile stress in the concrete is assumed to drop to zero. All other material parameters and convergence controls were identical for the three analyses. Loss of prestress occurs at about 0.55MPa and concrete cracking initiates at 0.75MPa. It is at this latter pressure that the behavior becomes dependent on the tension stiffening parameter used. As expected, the lower the tension stiffening, the more steep the slope of the post-cracking behavior. Higher values of tension stiffening result in a stiffer response of the containment. In this case, the analysis with the lowest tension stiffening failed to converge beyond the point of initial liner yielding at an internal pressure of 0.98MPa. The analysis with the intermediate value of tension stiffening failed to converge beyond an internal pressure of 1.10MPa. Only the analysis with a tension stiffening of 0.003 was able to converge beyond a pressure of 1.2MPa, which is when yielding begins in the hoop rebar in the upper middle section of the wall. The effects of hoop bar yielding can be seen in the change in slope at approximate 1.2MPa. This third analysis finally failed to converge when yielding in the hoop tendons initiates at a pressure of 1.29MPa. It should be noted that, based on the hardening characteristic of the rebar and tendons, hand calculations indicate a limit load for this containment of approximately 1.5MPa. Furthermore, the least ductile steel is in the hoop tendons with an elongation at failure of around 6%. (The rebar and liner are much more ductile.) However, at an internal pressure of 1.29MPa, the maximum hoop strain from the finite element results is only 0.5%.

The history of vertical displacement at the top of the containment is shown in Figure 5. In this case, the effects of the tension stiffening parameter can be seen beyond an internal pressure of 0.90MPa. This is the pressure at which extensive meridional cracks (crack face normal in hoop direction) occur. In all three analyses, the vertical deformation behavior at the top of the containment is very smooth throughout the loading. Even at an internal pressure of 1.29 MPA, no yielding has occurred in any vertical tendons or rebar, although yielding of the liner in the lower part of the dome begins by 1.20MPa.

The effects of concrete cracking and steel yielding on the convergence behavior of the code can be seen in Figure 6. Here the cumulative equilibrium iterations are plotted as a function of internal pressure for the three values of tension stiffening. The three analyses show identical convergence behavior up to an internal pressure of around 0.70MPa. Loss of prestress in the concrete occurs at 0.55MPa, and the concrete begins to crack by 0.70MPa. Because the tension stiffening parameter only affects behavior after cracking, it is at this pressure that the curves begin to diverge. After initial cracking, the number of iterations required for equilibrium increases for all three cases, but grows most rapidly for the analysis with the lowest tension stiffening.

Increases in the number of equilibrium iterations per increment of pressure also occur when yielding initiates in steel components of the structure. At an internal pressure of 0.96, the liner of the containment wall begins to yield. At this point, the time step is cut sharply for the analysis with the lowest value of tension stiffening, and by a pressure of 0.98MPa, this analysis is terminated because the time step becomes too small. For the intermediate value of tension stiffening, only a slight increase in iterations occurs at liner yielding. However, this analysis shows a sharp increase in iterations due to automatic cuts in the time step at a pressure just below 1.10MPa.

Finally, the analysis with a tension stiffening of 0.003 displays a sharp increase in iterations at the point of liner yielding at an internal pressure of 0.96 MPa, but continues to run. It should be noted that, in these analyses, the time step is only allowed to increase by a factor of 1.25 over the previous step so that once the time step is cut, it can only be increased slowly. The decreasing slope of

the iterations for the 0.003 curve from about 1.0MPa to 1.9Mpa reflects increasing time steps. At 1.19 MPa, the hoop rebar begins to yield causing more cuts in the time step and thus an increase in the iterations per increment of pressure. Increases in iteration counts also occur when yielding in the lower domes starts at 1.22MPa and when yielding initiates in the hoop tendons of the wall at 1.29MPa.

In all the analyses reported here, the convergence of the code was controlled by extensive use of the ***CONTROLS** options in ABAQUS Version 5.2. In general, the flexibility of these parameters greatly enhances the ability of the code to run problems involving concrete cracking with yielding of the steel components. Problems similar to the concrete containment analysis presented here were attempted with previous versions of ABAQUS. In those analyses, it was necessary to use the **DIRECT=NO STOP** parameter with a fixed, preset time step parameter to get any results at all. However, this method had at least two serious drawbacks. Foremost was that the user had no assurance of a "good" answer and had to be very diligent about reading the step convergence information in the **.DAT** file. Secondly, any time that the plasticity algorithm would fail to converge with the preset time interval, the code would automatically stop because cutting the time step was not allowed. Finally, the **DIRECT=NO STOP** option was very inefficient because the code was forced to iterate a preset number of times in every increment of the step, regardless of whether the residual had converged in fewer iterations. The new ***CONTROLS, PARAMETER=TIME INTEGRATION** option allows the user to set an upper limit on the number of iterations and then to force the code onto the next step (similar to the **DIRECT=NO STOP** option) while still allowing the code to cut the time step if needed for the plasticity algorithm. For these analyses, this was accomplished by setting a very loose alternative residual tolerance to be accepted after 15 equilibrium iterations while keeping the primary tolerance at a reasonable value.

The output time step and iteration information for the analysis with the highest tension stiffening shown in Table 1 illustrates the behavior of the code with the alternative residual tolerance and automatic time step control. Every time the number in the **ATT** (Attempts) column is greater than

1, the time step was automatically cut. In most cases in this analysis, these cuts correspond to the onset of plasticity in a steel component and messages to the effect that the plasticity algorithm failed to converge. Under the previous **DIRECT=NO STOP** method, the code would have immediately stopped the first time a cut in time step was attempted.

Secondly, a number of 15 or greater in the **EQUIL ITERS** column indicates an increment in which the alternative residual was accepted. Note that the alternative residual was required in only a very few of the increments. The vast majority of increments converged to the primary residual in far fewer than 15 iterations. Therefore the problem ran much more efficiently and, perhaps even more importantly, the analyst has some assurance as to the quality of the results.

One of the common features of all three analyses was the occasional drastic cut in time step size accompanied by the output message "**THE PLASTICITY ALGORITHM DID NOT CONVERGE AT xxx POINTS.**" Based on the internal pressures at which these messages occur, they seem to be associated with the onset of yielding in rebar subelements. However, this is only speculation since the message gives no indication of which elements are involved.

Even with the new ***CONTROLS** options and the 0.003 value of tension stiffening, the code was only able to compute out to an internal pressure of 1.29MPA at which pressure the code attempts to cut the time step below the minimum allowed. Difficulties in convergence in these regions where significant reductions in stiffness occur (in this case due to yielding) are typical of implicit codes. However, due to the hardening behavior of the rebar and tendon, the actual failure pressure may be as high as 1.5MPa at a maximum hoop strain of 6% associated with the limit of tendon elongation. It may be that computing all the way to the limit load in a reasonable amount of computation time may require an iterative method for solution.

Summary

By nature, implicit finite element codes have trouble converging during softening behavior which is inherent in the cracking of concrete and yielding of steel reinforcing. This paper summarizes experience in using ABAQUS Version 5.2 for computation of the response of a prestressed con-

crete containment vessel to severe internal pressures in an attempt to predict failure. Results from three analyses with different values for the ***TENSION STIFFENING** parameter in the concrete model were compared. In general, a higher value of the tension stiffening parameter makes the post-cracking behavior stiffer than a lower tension stiffening value, but also helps the convergence behavior. Results were obtained in the regime of rebar and tendon yielding only with the highest value (0.003) attempted for tension stiffening. The analyses with the two lower values failed to converge within the minimum specified time step at lower pressures.

Extensive use was made of the new ***CONTROLS** options in Version 5.2 of ABAQUS/Standard. The use of the alternative residual tolerance allowed the code to run much more efficiently with more assurance of valid results than the old method with the **DIRECT = NO STOP** parameter. Ultimately, however, the desire to predict failure will require computing even further into the plastic regime at a reasonable cost and may require an alternative method for solution.

References

[1] ABAQUS/Standard User's Manual, Version 5.2, Hibbitt, Karlsson & Sorensen, Inc., Pawtucket, RI, 1992.

Tables

Table 1. Summary of Job Information for Tension Stiffening = 0.003

STEP	INC	ATT	SEVERE DISCON ITERS	EQUIL ITERS	TOTAL ITERS	TOTAL TIME/ FREQ	STEP TIME/LPF	INC OF TIME/LPF
1	1	1	0	2	2	2.500E-04	2.500E-04	2.5000E-04
1	2	1	0	3	3	5.000E-04	5.000E-04	2.5000E-04
1	3	1	0	1	1	8.125E-04	8.125E-04	3.1250E-04
1	4	1	0	1	1	1.000E-03	1.000E-03	1.8750E-04
2	1	1	0	2	2	5.100E-02	5.000E-02	5.0000E-02
2	2	1	0	1	1	0.101	0.100	5.0000E-02
2	3	1	0	1	1	0.163	0.162	6.2500E-02
2	4	1	0	1	1	0.242	0.241	7.8125E-02
2	5	1	0	1	1	0.339	0.338	9.7656E-02
2	6	1	0	1	1	0.439	0.438	0.1000
2	7	1	0	1	1	0.501	0.500	6.1719E-02
3	1	1	0	2	2	0.521	2.000E-02	2.0000E-02
3	2	1	0	1	1	0.541	4.000E-02	2.0000E-02
3	3	1	0	1	1	0.566	6.500E-02	2.5000E-02
3	4	1	0	2	2	0.597	9.625E-02	3.1250E-02
3	5	1	0	1	1	0.636	0.135	3.9062E-02
3	6	1	0	2	2	0.685	0.184	4.8828E-02
3	7	1	0	7	7	0.735	0.234	5.0000E-02
3	8	2	0	6	6	0.760	0.259	2.5000E-02
3	9	1	0	4	4	0.791	0.290	3.1250E-02
3	10	1	0	6	6	0.830	0.329	3.9062E-02
3	11	1	0	9	9	0.879	0.378	4.8828E-02
3	12	1	0	11	11	0.929	0.428	5.0000E-02
3	13	2	0	3	3	0.954	0.453	2.5000E-02
3	14	4	0	1	1	0.957	0.456	3.1250E-03
3	15	3	0	4	4	0.958	0.457	9.7656E-04
3	16	3	0	1	1	0.959	0.458	3.0518E-04
3	17	1	0	14	14	0.959	0.458	3.8147E-04
3	18	1	0	2	2	0.959	0.458	3.8147E-04
3	19	1	0	2	2	0.960	0.459	3.8147E-04
3	20	1	0	1	1	0.960	0.459	4.7684E-04
3	21	1	0	2	2	0.961	0.460	5.9605E-04
3	22	1	0	2	2	0.962	0.461	7.4506E-04
3	23	1	0	2	2	0.963	0.462	9.3132E-04
3	24	1	0	2	2	0.964	0.463	1.1642E-03
3	25	1	0	1	1	0.965	0.464	1.4552E-03
3	26	1	0	9	9	0.967	0.466	1.8190E-03
3	27	1	0	5	5	0.969	0.468	2.2737E-03
3	28	1	0	2	2	0.972	0.471	2.8422E-03
3	29	1	0	4	4	0.976	0.475	3.5527E-03
3	30	1	0	5	5	0.980	0.479	4.4409E-03
3	31	1	0	8	8	0.986	0.485	5.5511E-03
3	32	1	0	4	4	0.993	0.492	6.9389E-03
3	33	1	0	7	7	1.00	0.500	8.3805E-03

Table 1. Continued

STEP	INC	ATT	SEVERE DISCON ITERS	EQUIL ITERS	TOTAL ITERS	TOTAL TIME/ FREQ	STEP TIME/LPF	INC OF TIME/LPF
4	1	1	0	15	15	1.02	2.000E-02	2.0000E-02
4	2	1	0	15	15	1.04	4.000E-02	2.0000E-02
4	3	1	0	15	15	1.06	6.000E-02	2.0000E-02
4	4	1	0	15	15	1.08	8.000E-02	2.0000E-02
4	5	1	0	6	6	1.10	0.100	2.0000E-02
4	6	1	0	6	6	1.12	0.120	2.0000E-02
4	7	1	0	4	4	1.15	0.145	2.5000E-02
4	8	1	0	4	4	1.18	0.176	3.1250E-02
4	9	3	0	5	5	1.19	0.186	9.7656E-03
4	10	1	0	4	4	1.20	0.198	1.2207E-02
4	11	5	0	18	18	1.20	0.199	9.5367E-04
4	12	2	0	4	4	1.20	0.200	4.7684E-04
4	13	1	0	4	4	1.20	0.200	4.7684E-04
4	14	1	0	2	2	1.20	0.201	5.9605E-04
4	15	1	0	2	2	1.20	0.201	7.4506E-04
4	16	1	0	2	2	1.20	0.202	9.3132E-04
4	17	1	0	3	3	1.20	0.204	1.1642E-03
4	18	1	0	2	2	1.21	0.205	1.4552E-03
4	19	1	0	3	3	1.21	0.207	1.8190E-03
4	20	1	0	2	2	1.21	0.209	2.2737E-03
4	21	1	0	2	2	1.21	0.212	2.8422E-03
4	22	1	0	2	2	1.22	0.216	3.5527E-03
4	23	2	0	2	2	1.22	0.218	2.2204E-03
4	24	5	0	2	2	1.22	0.218	3.9031E-04
4	25	1	0	5	5	1.22	0.219	4.8789E-04
4	26	2	0	11	11	1.22	0.219	4.5740E-04
4	27	1	0	3	3	1.22	0.220	4.5740E-04
4	28	1	0	2	2	1.22	0.220	4.5740E-04
4	29	1	0	2	2	1.22	0.221	5.7175E-04
4	30	1	0	2	2	1.22	0.221	7.1468E-04
4	31	1	0	2	2	1.22	0.222	8.9336E-04
4	32	1	0	2	2	1.22	0.223	1.1167E-03
4	33	1	0	1	1	1.23	0.225	1.3959E-03
4	34	1	0	2	2	1.23	0.226	1.7448E-03
4	35	1	0	2	2	1.23	0.229	2.1810E-03
4	36	1	0	2	2	1.23	0.231	2.7263E-03
4	37	1	0	2	2	1.24	0.235	3.4079E-03
4	38	1	0	5	5	1.24	0.239	4.2598E-03
4	39	1	0	9	9	1.25	0.244	5.3248E-03
4	40	1	0	3	3	1.25	0.251	6.6560E-03
4	41	1	0	2	2	1.26	0.259	8.3200E-03
4	42	2	0	3	3	1.27	0.264	5.2000E-03
4	43	1	0	15	15	1.27	0.271	6.5000E-03
4	44	1	0	8	8	1.28	0.277	6.5000E-03
4	45	1	0	7	7	1.28	0.284	6.5000E-03
4	46	2	0	15	15	1.29	0.288	4.0625E-03
4	47	5	0	6	6	1.29	0.288	3.8086E-04
4	48	3	0	9	9	1.29	0.289	9.5215E-05
4	49	2	0	13	13	1.29	0.289	8.9264E-05
4	50	1	0	4	4	1.29	0.289	8.9264E-05
4	51	1	0	1	1	1.29	0.289	8.9264E-05
4	52	1	0	1	1	1.29	0.289	1.1158E-04

Figures

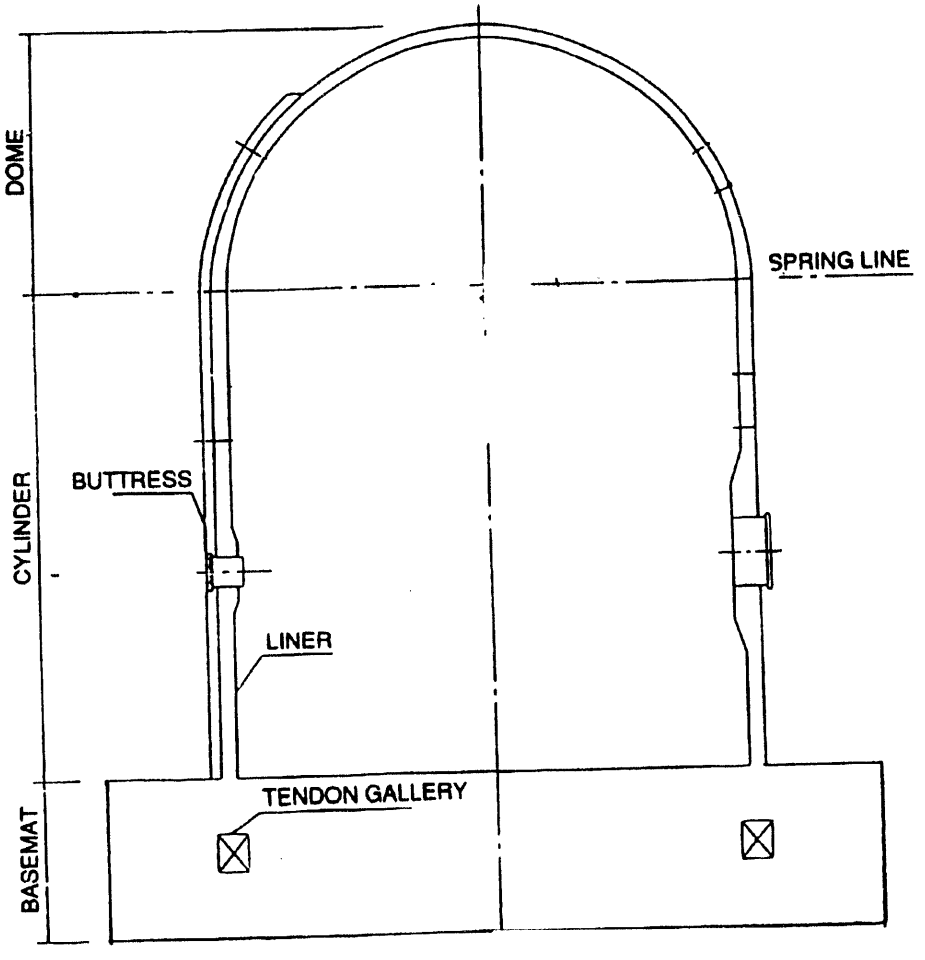

Figure 1. Schematic of prestressed concrete containment vessel.

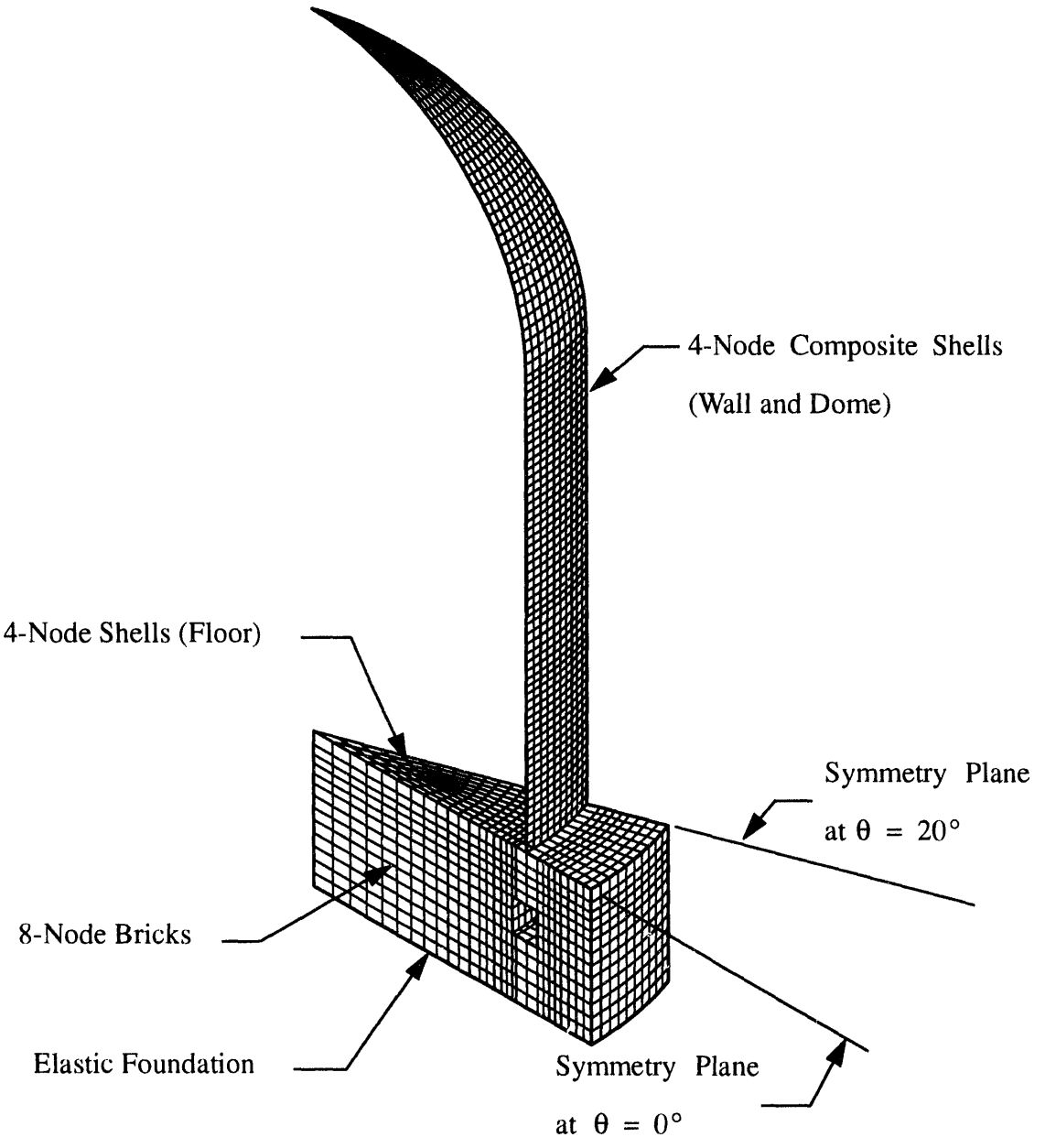

Figure 2. Finite element model of containment vessel.

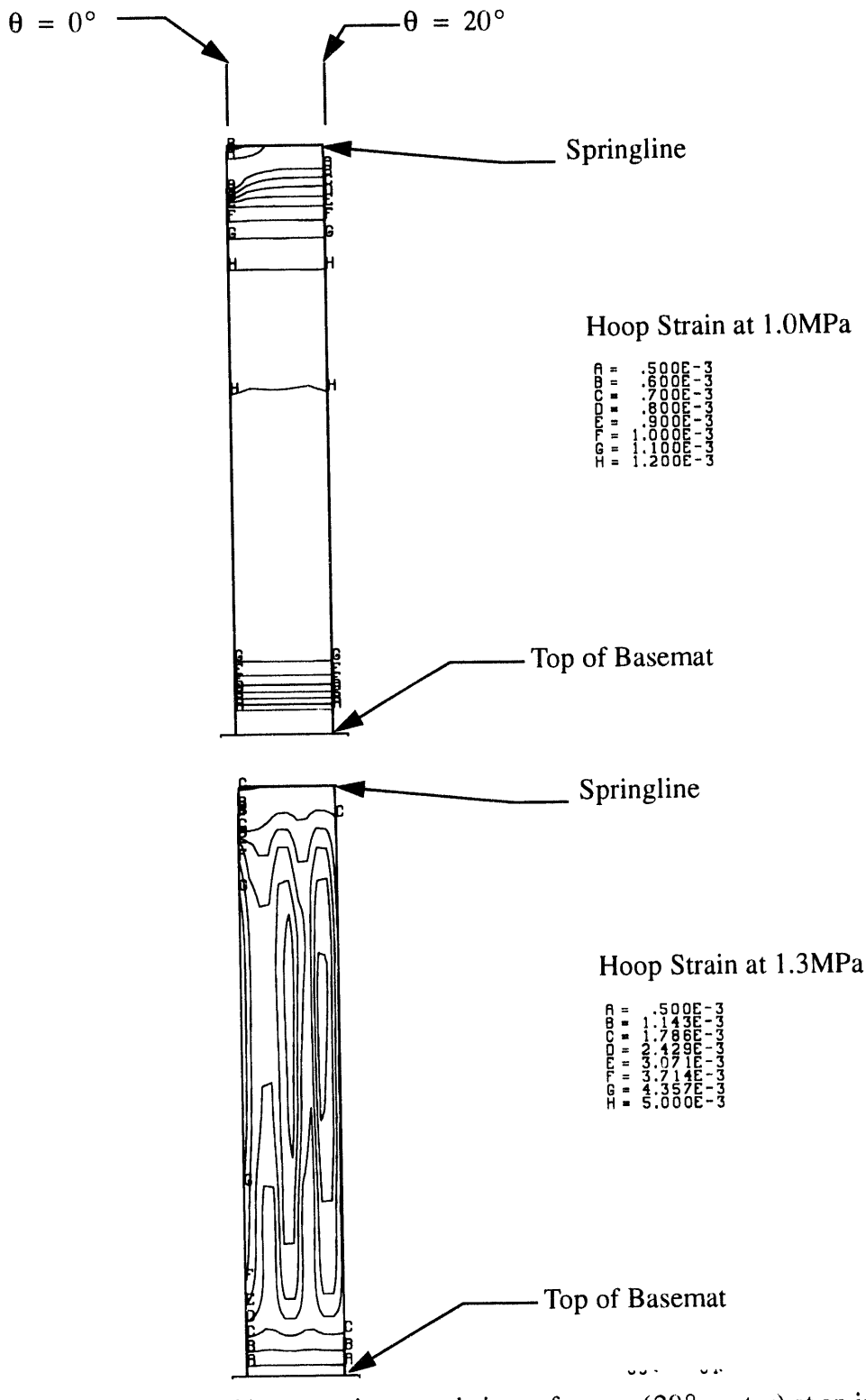

Figure 3. Distribution of hoop strain around circumference (20° sector) at an internal pressure of 1.0 and 1.3MPa.

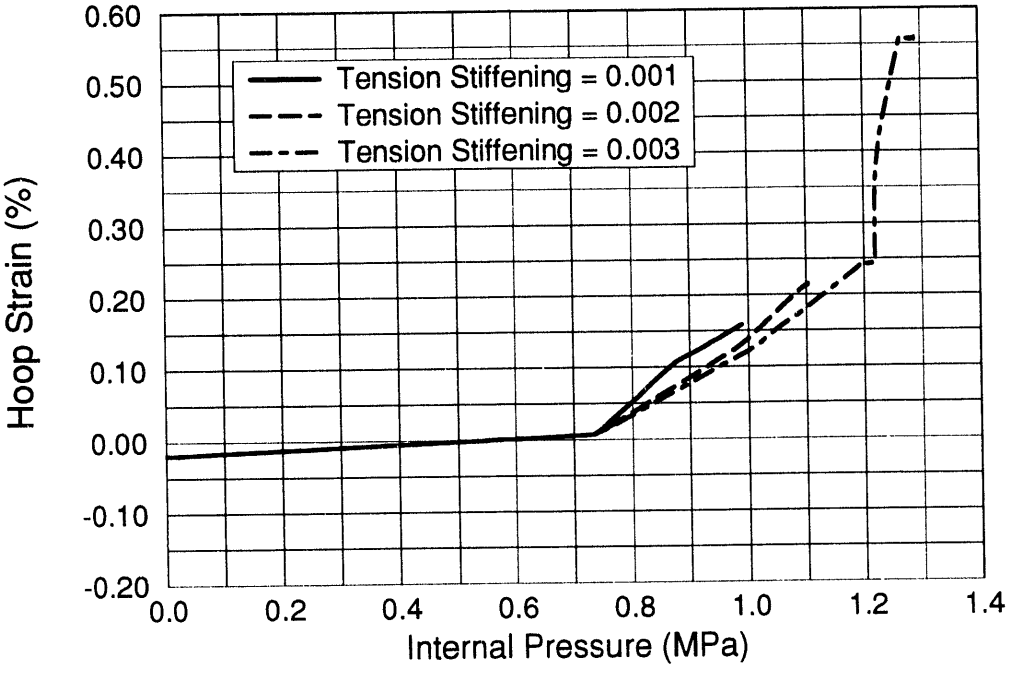

Figure 4. Hoop strain history in upper section of wall (location of maximum hoop strain).

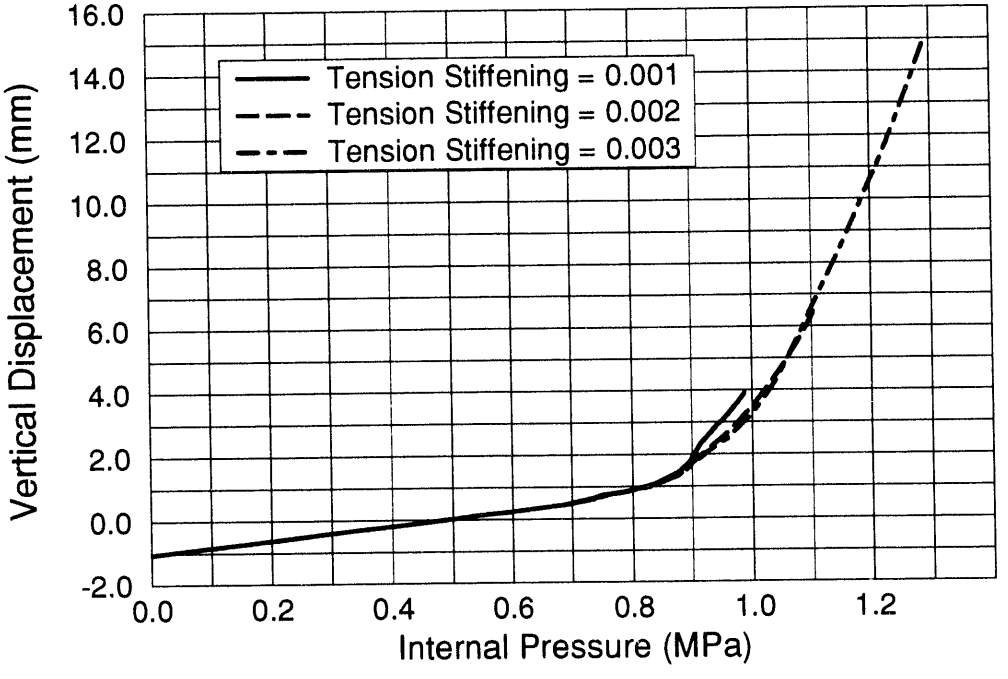

Figure 5. Vertical displacement at the top of the containment vessel.

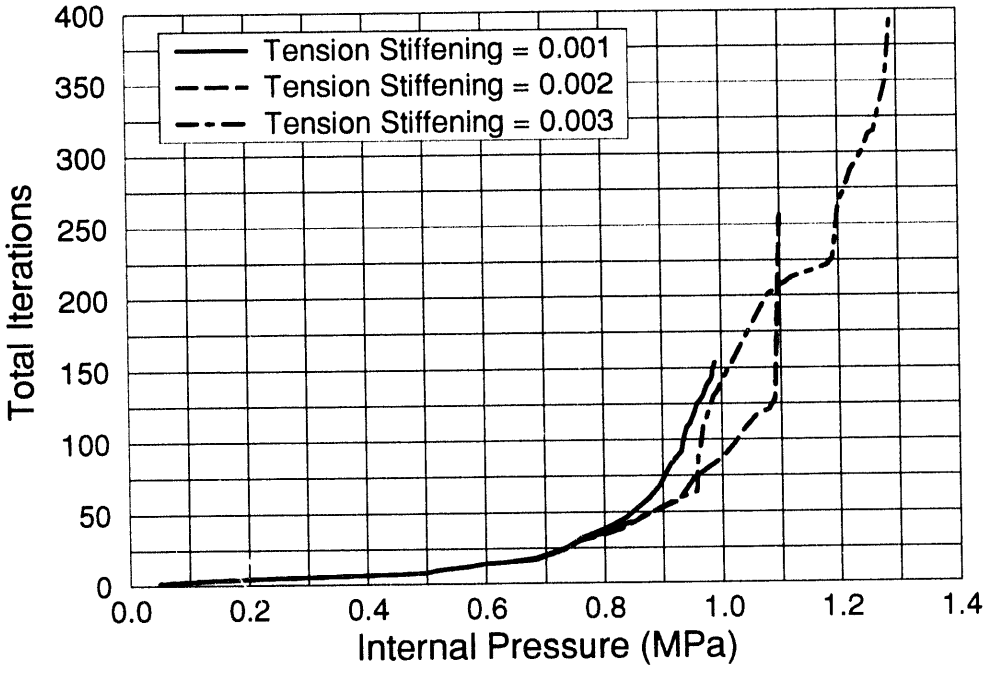

Figure 6. Cumulative number of equilibrium iterations.

DATE
FILMED
6/30/94

END